CivilEng

Review

Exploring Shear Wave Velocity—N_{SPT} Correlations for Geotechnical Site Characterization: A Review

Hasan Ali Abbas [1], Duaa Al-Jeznawi [2], Musab Aied Qissab Al-Janabi [2], Luís Filipe Almeida Bernardo [3,*] and Manuel António Sobral Campos Jacinto [4]

[1] Department of Building and Construction Techniques Engineering, Madenat Alelem University College, Baghdad 10006, Iraq; hassan_2007a@yahoo.com
[2] Department of Civil Engineering, College of Engineering, Al-Nahrain University, Jadriya, Baghdad 10070, Iraq; duaa.a.al-jeznawi@nahrainuniv.edu.iq (D.A.-J.); musab.a.jindeel@nahrainuniv.edu.iq (M.A.Q.A.-J.)
[3] Department of Civil Engineering and Architecture, University of Beira Interior, GeoBioTec-UBI, 6201-001 Covilhã, Portugal
[4] Civil Engineering Department, Polytechnic Institute of Guarda, 6300-559 Guarda, Portugal; jacinto@ipg.pt
* Correspondence: lfb@ubi.pt

Abstract: Shear wave velocity (V_s) is a critical parameter in geophysical investigations, micro-zonation research, and site classification. In instances where conducting direct tests at specific locations is challenging due to equipment unavailability, limited space, or initial instrumentation costs, it becomes essential to estimate V_s directly, using empirical correlations for effective site characterization. The present review paper explores the correlations of V_s with the standard penetration test (SPT) for geotechnical site characterization. V_s, a critical parameter in geotechnical and seismic engineering, is integral to a wide range of projects, including foundation design and seismic hazard assessment. The current paper provides a detailed analysis of the key findings, implications for geotechnical engineering practice, and future research needs in this area. It emphasizes the importance of site-specific calibration, the impact of geological background, depth-dependent behavior, data quality control, and the integration of V_s data with other geophysical methods. The review underlines the continuous monitoring of V_s values due to potential changes over time. Addressing these insights and gaps in research contributes to the accuracy and safety of geotechnical projects, particularly in seismic-prone regions.

Keywords: shear wave velocity (V_s); standard penetration test (SPT); empirical correlations; geophysical investigation; seismic wave; geotechnical applications; challenges and uncertainties

check for updates

Citation: Abbas, H.A.; Al-Jeznawi, D.; Al-Janabi, M.A.Q.; Bernardo, L.F.A.; Jacinto, M.A.S.C. Exploring Shear Wave Velocity—N_{SPT} Correlations for Geotechnical Site Characterization: A Review. *CivilEng* **2024**, *5*, 119–135. https://doi.org/10.3390/civileng5010006

Academic Editors: Mohammad Saberian Boroujeni and Akanshu Sharma

Received: 23 November 2023
Revised: 12 January 2024
Accepted: 17 January 2024
Published: 22 January 2024

1. Introduction

The accurate characterization of geotechnical properties at a construction site is a fundamental prerequisite for ensuring the stability and safety of underground geotechnical engineering projects. Several factors influence how destructive an earthquake can be, including its depth, magnitude, fault type, distance from the seismic source to the site, groundwater level, and local site conditions. The type of soil beneath a structure affects the behavior of ground movements during an earthquake between the depth of the bedrock and the surface. This is known as the local site effect [1]. The key characteristics of intense ground shaking, such as amplitude, frequency content, and duration, are significantly impacted by local site conditions. The degree of their influence is closely tied to the material properties of the subsurface [2]. Since earthquakes are difficult to predict, conducting a site-specific seismic hazard analysis is a practical approach in earthquake engineering [3]. One of the most crucial parameters for assessing the earthquake risk at a site is the shear wave velocity (V_s) specific to that location. The V_s value for the upper 30 m of soil is employed to estimate various dynamic properties of the soil [4–6]. Site-specific V_s characteristics provides insights into how the site is expected to respond during seismic shaking. V_s reflects the dynamic mechanical properties of subsurface materials and is instrumental in the assessment of soil and rock behavior under various load and environmental conditions [7]. According to Rajabi et al. [8], shear waves, also known as secondary or S-waves, are seismic waves that propagate through the earth's subsurface material, causing particles' movement to be perpendicular to the direction of wave propagation, as shown in Figure 1. Unlike compressional waves (P-waves), shear waves do not change the volume of the material but instead induce shear deformation (refer to Figure 1). It is a crucial parameter because it provides insights into the stiffness of geological formations [9]. It quantifies how quickly shear waves travel through the subsurface, which is directly related to the material's resistance to the dynamic shearing and deformation.

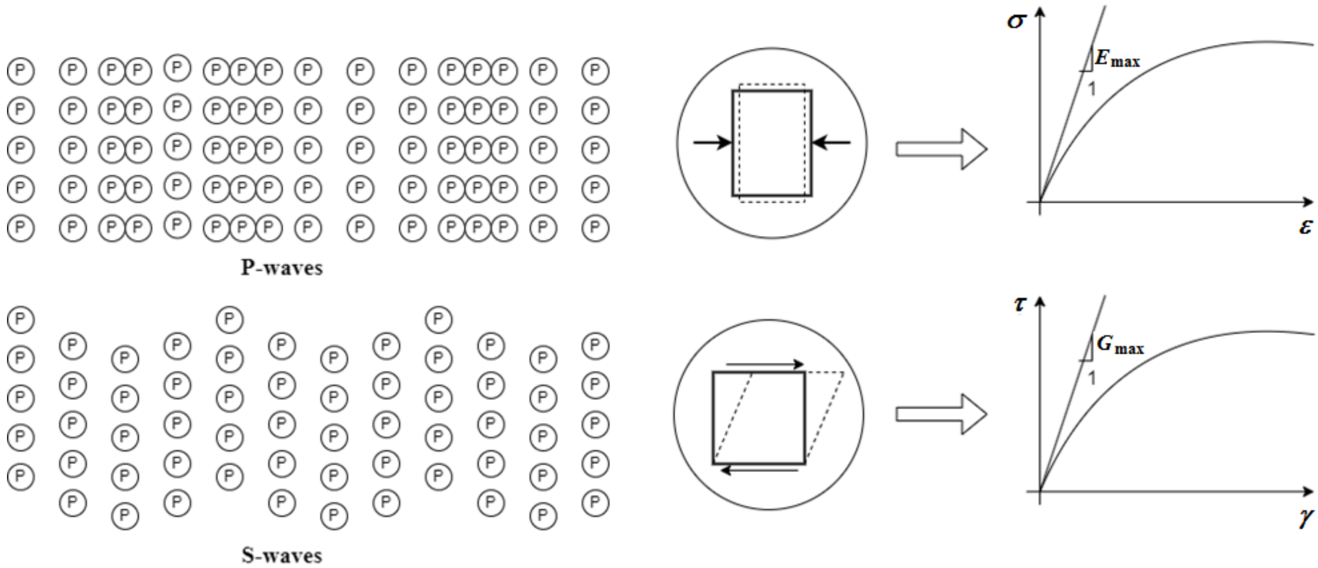

Figure 1. Visualizing the propagation of P and S seismic waves corresponding to stress–strain response and determination of the elastic modulus (E) in the case of P-waves, and the shear modulus (G) in the case of S-waves.

The proper determination of V_s can enhance our understanding of site-specific geotechnical challenges and contribute to the design and construction of resilient infrastructures. In recent years, the use of the standard penetration test (SPT) has been a common practice for assessing subsurface conditions and providing valuable data for geotechnical analysis. However, researchers and practitioners have increasingly recognized that SPT results alone may not always yield the most accurate representation of subsurface conditions, particularly in heterogeneous geological settings. This recognition has led to the exploration of alternative methods and correlations to refine the estimation of V_s [10].

The implementation of correlations in estimating V_s, particularly with respect to the SPT, is essential in geotechnical engineering. However, errors can occur due to factors influencing the choice of the correlation, such as the geological conditions, soil or rock type, and location, potentially leading to misleading estimations.

This paper focuses on the investigation of shear wave velocity correlations with the number of blows of the standard penetration test (N_{SPT}) for geotechnical site characterization. The N_{SPT} incorporates both dynamic and static measurements during soil penetration, providing a more comprehensive insight into the geotechnical properties of the subsurface. By examining the correlation between N_{SPT} results and V_s, this study aims to provide a critical discussion on the reliability of the former studies in estimating V_s by correlation, especially in regions where geological complexities pose significant challenges to traditional testing methods.

2. Significance of V_s in Geotechnical Engineering

V_s is incredibly important in geotechnical engineering because it has a central role in various aspects of the field [11]. The S-wave exclusively induces shear deformation (as shown in Figure 1), which is a key factor for understanding the elastic strength and stiffness of soil and rock layers below the surface, essentially providing a direct assessment of the material's rigidity and stiffness. This information is crucial for designing structures like foundations and retaining walls [12–14]. Additionally, V_s is essential for predicting how a site will respond during earthquakes, helping engineers design buildings that can withstand seismic activity. It also helps in designing foundations that can handle dynamic loads, such as those from wind, waves, and earthquakes [15]. Moreover, V_s is a cornerstone in assessing seismic hazards such as soil liquefaction [16]. It greatly contributes to evaluating earthquake risks, planning land use, creating building codes, and reducing risks [17]. Engineers rely on V_s data to make informed decisions about improving the ground, analyzing slope stability, planning tunnels and excavations, and assessing environmental impacts [18–21]. This ensures the safety and stability of various civil engineering projects, especially when dealing with seismic events and dynamic loads.

3. Role of N_{SPT} in V_s Determination

The N_{SPT} plays a significant role in V_s studies within geotechnical engineering. This test involves driving a standardized sampler into the ground and recording the number of blows required for it to penetrate a specific depth [22]. By driving a standardized sampler into the ground and recording penetration depths, N_{SPT} provides critical subsurface insights, allowing engineers to characterize soil and geological conditions [23]. The collected data are often taken at multiple depths, facilitating the creation of depth profiles that reveal variations in V_s with depth. Additionally, empirical correlations established between N_{SPT} values and V_s enable estimations of V_s in situations where direct measurements may be challenging or costly [1]. This information proves to be indispensable in regard to foundation design, aiding engineers in assessing material stiffness and the capacity to withstand dynamic loads, particularly during seismic events, thus ensuring the safety and stability of diverse civil engineering projects [24]. Furthermore, N_{SPT} data contribute significantly to seismic hazard assessments [25], as they offer valuable subsurface information that, when coupled with V_s data, help engineers evaluate a site's vulnerability to seismic events and rule the design of earthquake-resistant structures, ultimately enhancing risk mitigation strategies and land-use planning within geotechnical engineering.

Field and laboratory V_s measurements are commonly employed alongside other in situ tests such as the N_{SPT} and cone penetration resistance (q_c) by Cone Penetration Test (CPT), as well as laboratory measurements like effective confining pressure (σ') and void ratio (e) [26]. The V_s measurements are employed to create various correlations that can be incorporated into engineering research to harness the extensive data and expertise gathered by researchers [27]. While V_s values are generally preferred over estimates, correlations with penetration resistance can provide valuable and cost-effective insights in specific scenarios [28–32]:

- When constructing regional seismic hazard maps for site classification, using the average shear wave velocity down to a depth of 30 m (V_{s30}), the inclusion of correlations with penetration measurements can enhance the V_s values, especially because the range of V_{s30} values within each class is quite extensive.
- To offer validation for measured V_s values in scenarios demanding high accuracy in deposit response calculations, such as in studies related to liquefaction, it is advisable to confirm the consistency between geophysical and geotechnical measurements.
- As a preliminary tool for pinpointing areas where geophysical measurements would provide the most significant advantages.
- For initial assessments and rough estimations in low-risk projects where the expenses associated with comprehensive V_s testing are not warranted, either during feasibility studies or for the final design calculations.

- The V_s profile derived from correlations can serve as an initial input for commencing the inversion process in Rayleigh wave testing.

Recognizing their importance, it is important to mention that the reliability of numerous correlations used in engineering has been questioned. These correlations often overlook crucial factors that can significantly influence V_s values, such as variations in soil type, particle characteristics, geological age, and the initial fabric of the soil. For instance, both empirical findings and theoretical considerations have demonstrated that V_s is primarily influenced by e and σ'. One of the widely utilized empirical formulas for estimating (σ' and e) pairs is the one originally introduced by Hardin and Richart [33], and Hardin and Black [17]:

$$V_s = AF_e\,(\sigma')^B \tag{1}$$

where F_e represents a function based on the void ratio, and A and B are constants specific to the material. The stress exponent, denoted as B, ranges from 0.22 to 0.29, with many researchers endorsing a practical value of 0.25 [34]. However, classical contact mechanics solutions, based on the Hertz–Mindlin contact theory, predict a lower value for B at 0.16 [35]. This discrepancy arises from the assumption in these solutions that soil particles are smooth and behave like elastic spheres. When considering contacts involving rough surfaces, adjustments to the theory yield higher values of exponent B that better match the experimental findings [36]. The influence of effective stress is frequently eliminated by applying an overburden correction factor, as demonstrated in various studies (e.g., [37]). In essence, V_s is regularly adjusted to account for the vertical effective stress (${\sigma_v}'$), as observed in investigations aimed at assessing the liquefaction potential (e.g., [16,38]):

$$V_{s1} = V_s\left(\frac{Pa}{\sigma_v'}\right)^{0.25} \tag{2}$$

where V_{s1} represents the stress-normalized shear wave velocity, and Pa denotes normal atmospheric pressure in units consistent with ${\sigma_v}'$ (for instance, $Pa \approx 100$ kPa if ${\sigma_v}'$ is measured in kPa). The term $\left(\frac{Pa}{\sigma'_v}\right)^{0.25}$ is considered as a stress correction (C_{vs}) [16]. By substituting Equation (1) into Equation (2), the normalized shear wave velocity, V_{s1}, becomes as follows:

$$V_{s1} = AF_e\,(\sigma')^B\left(\frac{Pa}{{\sigma'}_v}\right)^{0.25} \tag{3}$$

When B is equal to 0.25, Pa is 100 kPa, and ${\sigma_v}' = \sigma'(3/(1 + 2K_0))$, with K_0 representing the coefficient of earth pressure at rest, the expression for V_{s1} can be formulated as follows:

$$V_{s1} = AF_e\left[\frac{100}{3/(1+2K_0)}\right]^{0.25} \tag{4}$$

These empirical relationships do not incorporate any function that considers particle characteristics, which encompass factors such as particle size, shape, gradation, and mineral composition. Additionally, these relationships do not establish any particle-size restrictions for the applicability of the proposed formula. Some researchers have made efforts to outline the key characteristics of various well-established correlations between V_s and parameters like N_{SPT}, q_c, relative density, mean grain size (D_{50}), and e [32]. This effort aims to aid readers in assessing the suitability of these correlations for practical applications in geotechnical engineering.

4. Measurement of V_s

V_s is determined for geomaterials by using laboratory tests or field (i.e., in situ) tests. The laboratory techniques are subdivided into the binder element test and resonant column test. The binder element test was developed by Shirley [39] and then Shirley and Hampton [40] to determine the shear velocity of the laboratory specimen scale of geomaterial at a very low shear strain <10^{-6} [41]. The shear velocity, as determined in this case, is based on two parameters, namely the wave traveling time and the specimen length. The boundary condition of length is the location of the pulser and the receiver transmitters, and the wave traveling time is defined as the first observed deflection in the time–amplitude graph [42]. However, many factors could affect the estimation of the traveling time, such as the moisture content [43], grain size [44], wave reflection [45], etc. Therefore, the frequency domain and cross-correlation are developed to reduce the uncertainties regarding the traveling time definition [46–49]. However, the outcomes of these techniques proved obvious deviations of V_s values following the soil type [50].

The resonant column test can be subclassified into several techniques depending on the specimen–setup–boundary condition and the vibration mode. The most popular setups are the fixed–free end and free–free end resonant column to measure both the longitudinal and torsional specimen vibration, as developed by Wilson [51] and Hardin and Richart [33], respectively. Drnevich, in 1985 [52], combined the resonant column and torsional shear into one device to identify the elastic characteristic of geomaterial with a strain range of 10^{-6}–10^{-1}. The wave velocity is determined using the resonant frequency domain and the coefficient of damping. The above laboratory methods are considered to be nondestructive tests dealing with elastic or elastic–plastic wave propagation. They are followed by many researches utilizing these techniques to characterize the elastic properties of soils [53–57] and rocks [58–61].

On the other hand, the in situ tests are either a surface geophysical technique or a combination of geotechnical investigation techniques with the geophysical technique for the subsurface. The surface seismic techniques are conducted at or near the ground level to investigate the subsurface characteristics indirectly depending on the reflected or refracted waves from the ground. Meanwhile, the subsurface involved in penetrating the ground to a specific depth is to be investigated using one of the geotechnical underground investigation methods, such as the borehole or the cone penetrometer test with attached seismic source and receiver. The seismic refraction is a geophysical method that depends on the Rayleigh surface waves, using the Spectral Analysis of Surface Waves (SASW) technique [62]. The shear velocity computed by the analysis of the refracted wave received depends on three parameters: travel times and the detector's and the source's locations [63].

The downhole logging test is widely used in the deep exploration of oil and minerals; it was developed by Schlumberger Educational Services, Texas [64]. The acoustic or sonic wave collected in this method by a group of receivers attached to an acoustic borehole logging probes moved down the borehole to be investigated, with the sonic wave source up the receiver by a specific distance [65,66]. The analysis of the received waves is carried out using the slowness travel time [67] or the frequency domain, using the Fast Fourier Transform (FFT) logarithm [68]. The cross-hole seismic test is relatively similar to that elaborated in the downhole logging test. However, in this test, the number of boreholes must be at least two or more to determine the V_s across the distance between the boreholes [69], where one of the boreholes contains the wave transmitter and the others works as wave receiver boreholes, as elaborated by standard D4428/D4428M-07 (2014) [70]. The V_s is calculated with the equation below:

$$V_s = SR/t_s \tag{5}$$

where SR is the distance between the source and receiver boreholes or between the two receiver boreholes, and t_s is the travel time of shear waves [71]. For a further assessment, the surface wave could be estimated as well by adopting the SASW or the Multichannel Analysis of Surface Waves (MASW) techniques [72,73]. The Seismic Cone Penetrometer Test (SCPT) is one of the common tests in geotechnical investigation to predict the elastic properties of geomaterial [74]. In this test, the cone penetration test is developed by adding a wave receiver inside the cone to determine the V_s at different depths generated by a wave source at the ground surface [75,76]. Since V_s is determined by defining the travel time of the wave, the attenuation of wave propagation may cause a huge dissipation in the shear wave. Therefore, the cross-correlation procedure can assist in identifying the traveling time [77]. However, using two arrays of seismic cones is a benefit to overcoming the issue of wave attenuation and determining the average V_s at an interval depth based on the following equation [78]:

$$V_s = (L_2 - L_1)/(T_2 - T_1) \quad (6)$$

where L_2 and L_1 are the calculated distances between the source and the deeper and shallower receiver, respectively. Meanwhile, T_2 and T_1 are the shear velocity wave travel time from the source to the deeper and shallower receiver, respectively. Table 1 presents a summary of laboratory and field tests to determine the V_s.

Table 1. A summary of laboratory and in situ tests to determine the Vs corresponding to the analysis method.

Test Type		Name	Analysis Method
Laboratory		Bender element	First arrival, frequency domain and cross-correlation
		Torsional resonant column test	Frequency domain by Fast Fourier Transformation (FFT)
In situ	Surface	Seismic refraction	Travel time analysis
		Seismic reflection	Reflection analysis by frequency domain and in time domain
	Subsurface	Downhole logging	First arrival, frequency domain
		Cross-hole seismic test	Travel time and amplitude analysis
		Seismic Cone Penetrometer Test (SCPT)	Travel time analysis, cross-correlation analysis

5. V_s-N_{SPT} Correlations

Obtaining V_s data at all intervals and in every borehole can be challenging due to various factors, such as financial constraints, noisy worksites, or a lack of expertise [79]. Consequently, a widely adopted approach for predicting V_s involves using correlations with other soil-related variables. These correlations were established based on factors like the N_{SPT}, depth (z), soil type (st), geological age, and overburden pressure, as identified in a number of research studies. Numerous variables can influence the N_{SPT} significantly. Among the most critical variables to consider are the type of hammer, the borehole diameter, the rod length, and the energy imparted to the tube with each hammer blow [80]. Correlations with the V_s are crucial in geotechnical engineering and seismic analysis, linking the V_s with other geotechnical or seismic parameters [81]. These correlations are essential for assessing soil and rock behavior during seismic events. N_{SPT}-based empirical correlations, specifically, establish relationships between the SPT results and V_s. These empirical correlations are developed through statistical analysis, allowing engineers to estimate V_s based on N_{SPT} values, often using data collected at various depths in a soil profile [82]. N_{SPT} consistently exhibits the strongest correlation with the V_s when compared to other variables. These correlations are typically expressed in the form of $V_s = aN^b$, where 'a' and 'b' represent coefficients specific to the site. Due to the increasing popularity of N_{SPT} in soil studies and the ease of collecting N_{SPT} data in most locations, these types of correlations are widely used. Several studies, such as the ones from Ghazi et al. [83] and Gautam [84], developed correlations between this geophysical variable and other physically determined soil parameters. Jafari, Shafiei, and Razmkhah [79] conducted a comprehensive assessment of the statistical relationship between the V_s and N_{SPT}. The majority of the studies they analyzed, except for Lee [24], specifically addressed the relationship between the uncorrected N_{SPT} and V_s across different soil types, including both sand and clay soils. These empirical correlations were typically developed for regions with similar lithological characteristics, taking into account regional variations in soil types and qualities resulting from diverse geological settings and ongoing geomorphic events. The scope of these correlations was primarily limited to equivalent geomorphic locations and soil attributes. Consequently, it remains essential to establish correlations between V_s and geotechnical characteristics by using data specific to particular locations, irrespective of the various proposed empirical relationships. Daag et al. [85] established an equation between the V_s and N_{SPT} through the application of a nonlinear regression approach. They developed equations linking these two variables within the Metro Manila region of the Philippines, utilizing 265 sets of N_{SPT} values corresponding to V_s data. The researchers assessed the accuracy of their models by using the R^2 statistic, yielding values within a range from 0.73 to 0.79. Hossain et al. [86] employed an indirect approach to develop a relationship between V_s and N_{SPT}, considering 13 different cities with varying soil components, including sand, clay, and silt. The study introduced an innovative technique for combining all the collected data and determining main correlations, specifically focusing on the Dinajpur city in Bangladesh. The study's assessment was conducted through the determination of R^2 values, which ranged from 0.04416 to 0.6134 for all soil types, 0.0593 to 0.668 for sand, 0.5911 to 0.7149 for clay, and 0.5547 to 0.6794 for silt. Naik et al. [87] developed an equation between N_{SPT} and V_s, using seismic downhole methods on 120 datasets across 12 different locations in Kanpur. Their findings indicated that the proposed correlation exhibited a strong performance, with a remarkable 95% of the data showing an error margin of only 10% of the scaled percentage error. The study evaluated the results in terms of R^2, which yielded values of approximately 0.898 and 0.927 for various soil types and clay, respectively. Hence, in this context, various researchers have proposed numerous correlations, which are summarized in Table 2.

The validation of these correlations involves field investigations where both N_{SPT} data and direct measurements of V_s are collected at specific sites [122]. These data are used to test the accuracy of the correlations by comparing predicted V_s values with measured V_s values. Zhang et al., in 2022 [123], stated that, while correlations offer cost-efficiency and rapid estimations of V_s, they also show limitations such as site-specific limitations, the range of applicable depths, and their dependence on soil types. Consequently, engineers usually use correlations as valuable tools, alongside site-specific investigations and direct measurements, to ensure accuracy in geotechnical assessments and project design.

Table 2. Relationships between V_s and N_{SPT} based on the previous works (note: $N \equiv N_{SPT}$).

No.	Reference	All Soil (m/s)	Sand (m/s)	Clay (m/s)
1	[85]	$56.82\ N^{0.4861}$	$45.07\ N^{0.5534}$	$70.26\ N^{0.4220}$
2	[88]	$99.5\ N^{0.345}$	$100.3\ N^{0.338}$	$94.4\ N^{0.379}$
3	[79]		$19\ N^{0.85}$	
4	[89]		$77.1\ N^{0.355}$	
5	[90]		$107.2\ N^{0.34}$	
6	[91]		$95\ N^{0.30}$	
7	[87]	$78.46\ N^{0.390}$		$81.18N^{0.377}$
8	[92]	$72\ N^{0.4}$		
9	[93]	$95.64\ N^{0.301}$	$100.53\ N^{0.265}$	
10	[94]	$58\ N^{0.39}$	$73\ N^{0.33}$	$44\ N^{0.48}$
11	[95]	$82.6\ N^{0.430}$	$79\ N^{0.434}$	
12	[96]	$90\ N^{0.309}$	$90.8\ N^{0.319}$	
13	[79]	$121\ N^{0.27}$	$80\ N^{0.33}$	
14	[97]	$68.3\ N^{0.292}$		
15	[98]	$22\ N^{0.85}$		
16	[99]	$19\ N^{0.6}$		
17	[99]	$51.5\ N^{0.516}$		
18	[100]		$123.4\ N^{0.29}$	$184.2\ N^{0.17}$
19	[101]	$107.6\ N^{0.36}$		
20	[102]		$162\ N^{0.17}$	$165.7\ N^{0.19}$
21	[103]	$121\ N^{0.27}$		
22	[104]	$76\ N^{0.33}$		
23	[24]		$157\ N^{0.49}$	$14\ N^{0.31}$
24	[105]		$125\ N^{0.3}$	
25	[106]	$116.1\ (N + 0.3185)^{0.202}$		

Table 2. *Cont.*

No.	Reference	All Soil (m/s)	Sand (m/s)	Clay (m/s)
26	[107]	$5.3\ N + 13$	$5.1N^{0.27} + 152$	
27	[108]		$100\ N^{0.29}$	
28	[109]		$56\ N^{0.5}$	
29	[110]	$97\ N^{0.314}$		
30	[111]	$61\ N^{0.5}$		
31	[112]		$80\ N^{0.333}$	$100\ N^{0.333}$
32	[113]	$85\ N^{0.348}$	$88\ N^{0.34}$	$94\ N^{0.34}$
33	[114]	$91\ N^{0.337}$		
34	[115]	$90\ N^{0.341}$		
35	[116]	$92\ N^{0.329}$		
36	[117]	$82\ N^{0.39}$	$59\ N^{0.47}$	
37	[118]		$87\ N^{0.87}$	
38	[119]	$92.1\ N^{0.33}$		
39	[120]	$85\ N^{0.31}$		
40	[104]	$76\ N^{0.33}$		
41	[121]		$32\ N^{0.5}$	
42	[99]	$N^{0.6}$		

6. Geotechnical Applications

The prediction of the geotechnical engineering of V_s has a variety of applications throughout the construction and infrastructure development process. By assisting engineers and geologists in understanding subsurface conditions, soil behavior, and seismic risks, this predictive capability eventually contributes to the safety and stability of structures [124]. It is essential to estimate the V_s while describing the characteristics of subsurface materials. Geotechnical engineers can categorize different types of soil and rock, gauge the stiffness of the soil, and recognize potential geohazards by measuring V_s values at various depths [125]. Poulos, in 2016 [126], stated that the accurate predictions of V_s are significant for engineers to adapt foundation designs to specific soil conditions, ensuring the stability of structures and infrastructure during site selection and foundation design processes. Predicting V_s, for instance, helps in determining the proper depth for deep foundations (such as piles or caissons) or the necessity for ground improvement procedures in places with soft or liquefiable soils, such as coastal zones [127]. Thus, when identifying the possibility of soil liquefaction during seismic occurrences, the V_s is a critical factor. Liquefaction is the temporary loss of strength of saturated soils, which can result in structural damage and the deterioration of foundations. Engineers may recognize liquefaction-prone regions by using predicted V_s profiles and then take mitigation steps to improve soil stability [128]. These steps might include ground densification or the installation of reinforcement. Therefore, it is important to predict V_s profiles in order to comprehend how seismic waves would travel through the subsurface. In areas with a high level of seismic activity, this information is essential for estimating the magnitude of ground vibrations and informing seismic design standards and building codes [129]. In order to customize rehabilitation procedures to specific soil conditions at various locations, Liu et al., in 2022 [130], emphasized the critical role of accurately predicting the V_s, as it is essential for assessing infrastructure resilience and facilitating modifications and reinforcements of older structures to meet current seismic safety standards. Also, Fang et al., in 2023 [131], emphasized that predicting V_s profiles is the key for tunnel lining design, excavation method selection, and overall ground stability estimation, reducing the probability of ground settlement and other geotechnical difficulties in tunneling and underground construction projects. Table 3 summarizes examples illustrating the dependency of geotechnical applications on V_s prediction.

Table 3. Examples of the dependency of geotechnical applications on V_s prediction.

No.	Geotechnical Application	V_s Role
1	Bridge design	Engineers evaluate the soil conditions at bridge piers by using estimated V_s values while building the foundations for bridges. The proper foundation type, depth, and design parameters could be determined using this information to guarantee the stability and safety of the bridge under a variety of loading circumstances, including seismic events [132].
2	Tunnel construction	Fang et al., in 2023 [131], stated that predicting V_s is crucial for tunnel lining construction, assessing tunneling project ground stability, avoiding subsidence, and optimizing excavation techniques to prevent tunnel collapses by providing insights into the geological conditions along the tunnel route.
3	Designing for earthquake hazard	Krinitzsky, in 1995 [133], stated that predicting V_s is a key for seismic hazard assessments, influencing earthquake hazard zoning, construction standards, and earthquake-resistant structure design in seismically active regions by helping determine ground motion predictions.
4	Dam safety	Ebrahimi et al., in 2022 [134], emphasized that engineers rely on accurate V_s data to assess dam stability, ensuring the development of safe and reliable dams capable of withstanding both typical loading and potential seismic events by examining foundational conditions.
5	Construction of underground utilities and pipelines	Chaudhuri and Choudhury, in 2023 [135], emphasized the importance of predicting V_s in the design of buried pipes and subsurface utilities, as it is essential for ensuring foundation stability and resilience against ground movements such as settlement or seismic activity in these structures.
6	Slope stability analysis	Yang et al., in 2023 [136], demonstrated that the prediction of V_s in geotechnical engineering is instrumental in assessing slope stability, allowing engineers to mitigate landslides and slope failures through a comprehensive understanding of subsurface conditions and soil shear strength in both natural and manmade slopes.
7	Landfill design	Valencia-González et al., in 2022 [137], emphasized that predicting V_s is crucial for evaluating the geotechnical properties of landfill liners and foundations to secure the environmentally safe containment of waste during landfill construction.
8	Coastal engineering	Munirwansyah et al., in 2020 [138], highlighted that the prediction of V_s is a key for the evaluation of the stability of coastal protective structures, including seawalls, revetments, and piers, thereby enabling engineers to design coastal defenses capable of withstanding waves and storm surge.
9	Mine planning	According to Allawi and Al-Jawad, in 2022 [124], the prediction of V_s in mining operations informs mining engineers about the geomechanical characteristics of surrounding rock, facilitating the design of secure and efficient mine slopes and tunnels.

7. Challenges and Uncertainties

Challenges in N_{SPT}-based V_s predictions arise from factors like soil variability, instrumentation quality, and depth limitations. These uncertainties can be addressed through site-specific analysis, high-quality equipment, and validation with other methods to improve reliability in geotechnical and seismic assessments.

7.1. Sources of Error in N_{SPT}-Based Vs Predictions

The measurement of V_s through the test of standard penetration is a valuable geotechnical tool, but it faces various challenges and uncertainties that can impact the accuracy of V_s estimates. Soil heterogeneity, characterized by variations in soil types, compaction, and layering across a site, can introduce substantial errors in N_{SPT}-derived V_s measurements, thereby compromising the accuracy of V_s estimations. Instrumentation quality and calibration discrepancies in N_{SPT} equipment can vary, potentially impacting the dependability of V_s measurements and introducing errors through calibration issues, sensor errors, or improper equipment use [139]. The depth to which V_s is measured in N_{SPT}, primarily focusing on upper soil layers, may not accurately represent deeper strata, potentially introducing errors in geotechnical designs, particularly in cases where deep-seated soil conditions are important [140]. Tunusluoglu, in 2023 [141], stated that empirical correlations used for converting N_{SPT} data to V_s introduce uncertainty, as they are often based on local or regional data and may not be universally applicable across diverse geological situations. Inaccurate V_s profiles can result from insufficient spacing and depth of N_{SPT} investigations, while the presence of varying soil layers and interfaces may introduce errors through shear wave reflection or refraction in V_s measurements [142]. Verstraeten et al., in 2008 [143], discussed that environmental conditions, such as soil moisture content, temperature, and groundwater levels, can affect the propagation of shear waves, introducing uncertainties into V_s measurements. Nejad et al., in 2017 [144], demonstrated that the restrictions on the depth to which shear waves can propagate in N_{SPT} testing, often dictated by the rod's length, might require the adoption of more advanced geophysical techniques to obtain deeper V_s information, which can potentially introduce errors during the transition from N_{SPT} to these methods. Al-Jeznawi et al., in 2023 [82], highlighted that site-specific geological factors, such as the presence of unconsolidated sediments, bedrock, or faults, can create complex subsurface conditions that make it challenging to assess V_s accurately through N_{SPT} testing. Furthermore, variability in data inversion techniques for N_{SPT} data to derive V_s profiles can affect the quality of the results, with errors potentially arising from inappropriate model assumptions or insufficient data processing [145].

7.2. Data Interpretation Challenges of Vs in Terms of N_{SPT}

Interpreting V_s through the SPT data involves various challenges and uncertainties affecting the reliability of the results [146]. One significant challenge is the dependence on empirical correlations for V_s estimation, which may not be commonly applicable and can introduce errors, especially when applied beyond their original region of development. Soil behavior can be highly variable even within a single geological formation, making it essential to account for local geological situation and soil property variations during interpretation [141]. Furthermore, the influence of soil types on V_s estimations must be carefully considered, as different soil types exhibit different responses to SPT testing. Paoletti, in 2012 [147], emphasized the significance of sampling depth, especially in heterogeneous soil profiles where deeper sampling may be essential for accurate characterization of deeper strata, while also highlighting the potential introduction of uncertainties in the interpretation of SPT results due to factors like hammer energy and borehole condition. Ensuring data quality is a key, given that imprecisions in data collection, such as miscounts or equipment errors, have the potential to undermine the reliability of V_s estimates [140]. Additionally, interpreting V_s values is further complicated by the depth-dependent characteristics of soil; dynamic effects from the SPT hammer impact; and geological complexity, particularly in areas with faults, rock layers, or mixed soil types [88]. Therefore, the integration of data from multiple SPT tests, carried out at different site locations, frequently presents challenges that require thorough consideration and interpretation.

8. Case Studies

V_s derived from the N_{SPT} has found extensive applications in geotechnical and seismic engineering [141]. Real-world case studies demonstrate the invaluable role of N_{SPT}-derived V_s in various scenarios. For instance, in seismic-prone regions like California, comprehending and characterizing subsurface V_s profiles is a key for earthquake engineering and hazard assessment [148]. The latter has stated that the seismic performance of structures and sites exposed to earthquakes is complicatedly linked to these V_s profiles. Thus, to ensure the resilience of buildings and infrastructure in California, engineers usually employ N_{SPT}-derived V_s values. These data are fundamental for evaluating the dynamic response of the ground during seismic events, including the propagation of seismic waves through soil and their interaction with structures. Several case studies demonstrate the practical use of N_{SPT}-derived V_s values, involving evaluations at a variety of sites, including urban areas, fault zones, and regions with different geological characteristics.

Idriss and Boulanger, in 2006 [149], explored the varying roles of liquefaction correlations based on different testing methods, such as SPT, CPT, and V_s. For instance, fluctuating the relative density (D_r) of a clean sand from 30% to 80% is expected to result in a considerable increase in N_{SPT}, estimated to be approximately 7.1 times higher, and a substantial rise in CPT tip resistance, approximately 3.3 times higher, as indicated by Equations (7) and (8), respectively. According to the available correlations, the same change in D_r was expected to impact V_s, increasing it by a factor of about 1.4.

$$D_r = \sqrt{\frac{(N_1)_{60}}{40}} \tag{7}$$

$$D_r = 0.478\ (q_{CIN})^{0.264} - 1.063 \tag{8}$$

where q_{CIN} is q_C/Pa, as suggested by Robertson and Wride in 1997 [150]; q_C is the cone tip resistance; and Pa is the atmospheric pressure.

As an illustration, Seed, in 1970 [151], proposed that the parameter $K_{2\max}$ would equal 34 and 64 for a D_r of 30% and 80%, respectively. This results in V_s values that differ by a factor of approximately the square root of 64 divided by 34, which is about 1.37. The authors stated that it is possible that this range could be somewhat greater in the case of soils with a significant gravel content. Consequently, there is an ongoing requirement for a more comprehensive understanding of correlations based on V_s and an evaluation of their precision in comparison to correlations based on SPT and CPT data.

Other case studies highlighted the practical application of V_s data derived from the N_{SPT} in ensuring the stability, safety, and long-term performance of critical structures (tall buildings and bridges). This was comprehensively discussed by Yeung and Kitch [152], and Tomlinson and Woodward [153]. Ensuring the resilience of critical infrastructure, such as pipelines and lifelines, was addressed by Seed in 1970 [151], Whitman and Liao in 1985 [154], and Kramer in 1996 [2], who considered one of the primary concerns in earthquake-prone areas, namely the potential for ground shaking to damage or disrupt critical infrastructure. Pipelines that transport water, gas, or petroleum, as well as lifelines like power distribution systems, communication networks, and transportation routes, are exclusively susceptible.

A number of case studies have highlighted the wide range of applications of V_s obtained through the N_{SPT} in practical settings. N_{SPT}-derived V_s values offer important information on subsurface conditions and soil behavior, significantly impacting the fields of geotechnical and seismic engineering. These applications lead to enhanced safety and resilience in construction practices.

Practically, predicting the V_s from SPT tests should include the significance of site-specific calibration to account for varying geological conditions, the crucial role of geological background in V_s predictions, the depth-dependent behavior of soil and the need for comprehensive depth profiles, the direct relationship between data quality and reliable V_s estimations, the value of integrating N_{SPT}-derived V_s with other geophysical methods, and the importance of continuous monitoring due to potential V_s changes over time, all contributing to the precision and reliability of V_s predictions.

9. Conclusions

This review paper provides a comprehensive overview of V_s-N_{SPT} correlations, highlighting their essential role in geotechnical and seismic engineering applications. The key findings underscore the significance of site-specific calibration, geological background, depth-dependent behavior, data quality, and integration with other geophysical methods in ensuring the accuracy of V_s predictions. Continuous monitoring is emphasized to account for potential changes in V_s values over time. The implications for geotechnical engineering practice necessitate the need for systematic calibration, data quality assurance, and an integrated approach to V_s estimations. In geotechnical engineering, addressing uncertainties in V_s estimation is crucial for project safety and success. This involves site-specific investigations, data quality control, advanced techniques, considering various factors, accounting for depth-dependent behavior, and minimizing errors. Risk assessments and professional guidance are essential for reliable geotechnical projects, even in unpredictable subsurface conditions. The current review identifies research gaps in the development of stronger correlations, the improvement of depth-dependent models, and the exploration of innovative techniques, providing a roadmap for advancing V_s prediction methods in the field.

Author Contributions: Data collection, D.A.-J.; investigation, M.A.Q.A.-J.; writing—review and editing, D.A.-J. and H.A.A.; review and writing—original draft preparation, L.F.A.B. and M.A.S.C.J.; review, editing, and visualization, H.A.A., M.A.Q.A.-J., M.A.S.C.J. and L.F.A.B. All authors have read and agreed to the published version of the manuscript.

Funding: This research received no external funding.

Institutional Review Board Statement: Not applicable.

Informed Consent Statement: Not applicable.

Data Availability Statement: All the data used to support the findings of this study are included within the article.

Conflicts of Interest: The authors declare no conflicts of interest.

References

1. Kishida, T.; Tsai, C.-C. Prediction model of shear wave velocity by using SPT blow counts based on the conditional probability framework. *J. Geotech. Geoenviron. Eng.* **2017**, *143*, 04016108. [CrossRef]
2. Kramer, S.L. *Geotechnical Earthquake Engineering*; Pearson Education India: Noida, India, 1996.
3. Wang, J.; Taheri, H. Seismic hazard assessment of the Tehran region. *Nat. Hazards Rev.* **2014**, *15*, 121–127. [CrossRef]
4. Sil, A.; Sitharam, T. Dynamic site characterization and correlation of shear wave velocity with standard penetration test 'N' values for the city of Agartala, Tripura state, India. *Pure Appl. Geophys.* **2014**, *171*, 1859–1876. [CrossRef]
5. Duan, J.; Asteris, P.G.; Nguyen, H.; Bui, X.-N.; Moayedi, H. A novel artificial intelligence technique to predict compressive strength of recycled aggregate concrete using ICA-XGBoost model. *Eng. Comput.* **2021**, *37*, 3329–3346. [CrossRef]
6. Naji, D.M.; Akin, M.K.; Cabalar, A.F. Evaluation of seismic site classification for Kahramanmaras City, Turkey. *Environ. Earth Sci.* **2021**, *80*, 97. [CrossRef]
7. Gholami, A.; Amirpour, M.; Ansari, H.R.; Seyedali, S.M.; Semnani, A.; Golsanami, N.; Heidaryan, E.; Ostadhassan, M. Porosity prediction from pre-stack seismic data via committee machine with optimized parameters. *J. Pet. Sci. Eng.* **2022**, *210*, 110067. [CrossRef]
8. Rajabi, M.; Hazbeh, O.; Davoodi, S.; Wood, D.A.; Tehrani, P.S.; Ghorbani, H.; Mehrad, M.; Mohamadian, N.; Rukavishnikov, V.S.; Radwan, A.E. Predicting shear wave velocity from conventional well logs with deep and hybrid machine learning algorithms. *J. Pet. Explor. Prod. Technol.* **2023**, *13*, 19–42. [CrossRef]
9. Akhundi, H.; Ghafoori, M.; Lashkaripour, G.-R. Prediction of shear wave velocity using artificial neural network technique, multiple regression and petrophysical data: A case study in Asmari reservoir (SW Iran). *Open J. Geol.* **2014**, *4*, 303–313. [CrossRef]
10. Liu, Y.; Chen, Z.; Hu, K. Shear velocity prediction and its rock mechanic implications. In Proceedings of the EG/CWLS GeoConvention 2012, (Vision) Calgary TELUS Convention Centre & ERCB Core Research Centre, Calgary, AB, Canada, 14–18 May 2012.
11. Baghbani, A.; Choudhury, T.; Costa, S.; Reiner, J. Application of artificial intelligence in geotechnical engineering: A state-of-the-art review. *Earth-Sci. Rev.* **2022**, *228*, 103991. [CrossRef]
12. Choi, Y.; Stewart, J.P. Nonlinear site amplification as function of 30 m shear wave velocity. *Earthq. Spectra.* **2005**, *21*, 1–30. [CrossRef]
13. Patel, A.; Bartake, P.; Singh, D. An empirical relationship for determining shear wave velocity in granular materials accounting for grain morphology. *Geotech. Test. J.* **2008**, *32*, 1–10. [CrossRef]
14. Lee, C.-J.; Hung, W.-Y.; Tsai, C.-H.; Chen, T.; Tu, Y.; Huang, C.-C. Shear wave velocity measurements and soil–pile system identifications in dynamic centrifuge tests. *Bull. Earthq. Eng.* **2014**, *12*, 717–734. [CrossRef]
15. McGillivray, A.; Mayne, P.W. Seismic piezocone and seismic flat dilatometer tests at Treporti. In Proceedings of the ISC-2 on Geotechnical and Geophysical Site Characterization, Porto, Portugal, 19–22 September 2004; pp. 1695–1700.

16. Kayen, R.; Moss, R.; Thompson, E.; Seed, R.; Cetin, K.; Kiureghian, A.D.; Tanaka, Y.; Tokimatsu, K. Shear-wave velocity–based probabilistic and deterministic assessment of seismic soil liquefaction potential. *J. Geotech. Geoenviron. Eng.* **2013**, *139*, 407–419. [CrossRef]
17. Hardin, B.O.; Black, W.L. Sand stiffness under various triaxial stresses. *J. Soil. Mech. Found. Div.* **1966**, *92*, 27–42. [CrossRef]
18. Abuel-Naga, H.M.; Bouazza, A. Numerical experiment-artificial intelligence approach to develop empirical equations for predicting leakage rates through GM/GCL composite liners. *Geotext. Geomembr.* **2014**, *42*, 236–245. [CrossRef]
19. Sahebzadeh, S.; Heidari, A.; Kamelnia, H.; Baghbani, A. Sustainability features of Iran's vernacular architecture: A comparative study between the architecture of hot–arid and hot–arid–windy regions. *Sustainability* **2017**, *9*, 749. [CrossRef]
20. Rashid, Q.A.; Abuel-Naga, H.; Leong, E.-C.; Lu, Y.; Al Abadi, H. Experimental-artificial intelligence approach for characterizing electrical resistivity of partially saturated clay liners. *Appl. Clay Sci.* **2018**, *156*, 1–10. [CrossRef]
21. Feng, Y.; Wang, J.; Bai, Z.; Reading, L. Effects of surface coal mining and land reclamation on soil properties: A review. *Earth-Sci. Rev.* **2019**, *191*, 12–25. [CrossRef]
22. Gibbs, H.J. Research on determining the density of sands by spoon penetration testing. In Proceedings of the 4th International Conference on Soil Mechanics and Foundation Engineering, London, UK, 12–24 August 1957.
23. Anbazhagan, P.; Parihar, A.; Rashmi, H. Review of correlations between SPT N and shear modulus: A new correlation applicable to any region. *Soil. Dyn. Earthq. Eng.* **2012**, *36*, 52–69. [CrossRef]
24. Lee, S.H.-H. Analysis of the multicollinearity of regression equations of shear wave velocities. *Soils Found.* **1992**, *32*, 205–214. [CrossRef]
25. Cetin, K.O.; Seed, R.B.; Kayen, R.E.; Moss, R.E.; Bilge, H.T.; Ilgac, M.; Chowdhury, K. SPT-based probabilistic and deterministic assessment of seismic soil liquefaction triggering hazard. *Soil Dyn. Earthq. Eng.* **2018**, *115*, 698–709. [CrossRef]
26. Kumar, D.R.; Samui, P.; Burman, A. Determination of best criteria for evaluation of liquefaction potential of soil. *Transp. Infrastruct. Geotechnol.* **2022**, *10*, 1345–1364. [CrossRef]
27. Sykora, D.W. *Examination of Existing Shear Wave Velocity and Shear Modulus Correlations in Soils*; US Army Engineer Waterways Experiment Station: Washington, DC, USA, 1987.
28. Gazetas, G. *Foundation Vibrations. Foundation Engineering Handbook*; Van Nostrand Reinhold: New York, NY, USA, 1991; pp. 553–593.
29. Andrus, R.D.; Mohanan, N.P.; Piratheepan, P.; Ellis, B.S.; Holzer, T.L. Predicting shear-wave velocity from cone penetration resistance. In Proceedings of the 4th International Conference on Earthquake Geotechnical Engineering, Thessaloniki, Greece, 25–28 June 2007.
30. Wichtmann, T.; Triantafyllidis, T. Influence of the grain-size distribution curve of quartz sand on the small strain shear modulus G max. *J. Geotech. Geoenviron. Eng.* **2009**, *135*, 1404–1418. [CrossRef]
31. Brandenberg, S.J.; Bellana, N.; Shantz, T. Shear wave velocity as function of standard penetration test resistance and vertical effective stress at California bridge sites. *Soil Dyn. Earthq. Eng.* **2010**, *30*, 1026–1035. [CrossRef]
32. Karray, M.; Lefebvre, G.; Ethier, Y.; Bigras, A. Influence of particle size on the correlation between shear wave velocity and cone tip resistance. *Can. Geotech. J.* **2011**, *48*, 599–615. [CrossRef]
33. Hardin, B.O.; Richart, F., Jr. Elastic wave velocities in granular soils. *J. Soil Mech. Found. Div.* **1963**, *89*, 33–65. [CrossRef]
34. Bui, M.T. *Influence of Some Particle Characteristics on the Small Strain Response of Granular Materials*; University of Southampton: Gelang Patah, Malaysia, 2009.
35. Santamarina, J.C.; Klein, A.; Fam, M.A. Soils and waves: Particulate materials behavior, characterization and process monitoring. *J. Soils Sediments* **2001**, *1*, 130. [CrossRef]
36. Yimsiri, S.; Soga, K. Micromechanics-based stress–strain behaviour of soils at small strains. *Géotechnique* **2000**, *50*, 559–571. [CrossRef]
37. Skempton, A. Standard penetration test procedures and the effects in sands of overburden pressure, relative density, particle size, ageing and overconsolidation. *Géotechnique* **1986**, *36*, 425–447. [CrossRef]
38. Youd, T.L.; Idriss, I.M. Liquefaction resistance of soils: Summary report from the 1996 NCEER and 1998 NCEER/NSF workshops on evaluation of liquefaction resistance of soils. *J. Geotech. Geoenviron. Eng.* **2001**, *127*, 297–313. [CrossRef]
39. Shirley, D.J. An improved shear wave transducer. *J. Acoust. Soc. Am.* **1978**, *63*, 1643–1645. [CrossRef]
40. Shirley, D.J.; Hampton, L.D. Shear-wave measurements in laboratory sediments. *J. Acoust. Soc. Am.* **1978**, *63*, 607–613. [CrossRef]
41. Ali, H. *Study of Laboratory and Field Techniques to Measure Shear Wave Parameters-Frequency Effects*; University of Waterloo: Waterloo, ON, Canada, 2015.
42. Jovičić, V.; Coop, M.; Simić, M. Objective criteria for determining G max from bender element tests. *Géotechnique* **1996**, *46*, 357–362. [CrossRef]
43. Irfan, M.; Uchimura, T. Effects of soil moisture on shear and dilatational wave velocities measured in laboratory triaxial tests. In Proceedings of the 5th International Young Geotechnical Engineers' Conference, Marne-la-Vallée, France, 31 August–1 September 2013; pp. 505–509.
44. Russo, B.M.; Athanasopoulos-Zekkos, A.; Kim, J. Effect of Grain Size of Granular Soils on Shear Wave Velocity and Electrical Resistivity for Levee Health Monitoring. In Proceedings of the Geo-Congress 2023, Los Angeles, CA, USA, 26–29 March 2023; pp. 415–423.

45. Lindh, P.; Lemenkova, P. Ultrasonic P-and S-Wave Reflection and CPT Soundings for Measuring Shear Strength in Soil Stabilized by Deep Lime/Cement Columns in Stockholm Norvik Port. *Arch. Acoust.* **2023**, *48*, 325–346. [CrossRef]
46. Viggiani, G.; Atkinson, J. Interpretation of bender element tests. *Géotechnique* **1995**, *45*, 149–154. [CrossRef]
47. Brocanelli, D.; Rinaldi, V. Measurement of low-strain material damping and wave velocity with bender elements in the frequency domain. *Can. Geotech. J.* **1998**, *35*, 1032–1040. [CrossRef]
48. Blewett, J.; Blewett, I.; Woodward, P. Measurement of shear-wave velocity using phase-sensitive detection techniques. *Can. Geotech. J.* **1999**, *36*, 934–939. [CrossRef]
49. Lee, J.-S.; Santamarina, J.C. Bender elements: Performance and signal interpretation. *J. Geotech. Geoenviron. Eng.* **2005**, *131*, 1063–1070. [CrossRef]
50. Ogino, T.; Kawaguchi, T.; Yamashita, S.; Kawajiri, S. Measurement deviations for shear wave velocity of bender element test using time domain, cross-correlation, and frequency domain approaches. *Soils Found.* **2015**, *55*, 329–342. [CrossRef]
51. Wilson, S.D. Effect of consolidation pressure on elastic and strength properties of clay. In Proceedings of the ASCE Research Conference on Shear Strength of Cohesive Soils, New York, NY, USA, June 1960; pp. 419–435. Available online: https://cir.nii.ac.jp/crid/1571135649476007040 (accessed on 31 October 2023).
52. Drnevich, V.P. Recent developments in resonant column testing. In Proceedings of the Richart Commemorative Lectures, Detroit, MI, USA, 23 October 1985; pp. 79–107.
53. Hicher, P.-Y. Elastic properties of soils. *J. Geotech. Eng.* **1996**, *122*, 641–648. [CrossRef]
54. Jovičić, V.; Coop, M. The measurement of stiffness anisotropy in clays with bender element tests in the triaxial apparatus. *Geotech. Test. J.* **1998**, *21*, 3–10. [CrossRef]
55. Kumar, J.; Madhusudhan, B. On determining the elastic modulus of a cylindrical sample subjected to flexural excitation in a resonant column apparatus. *Can. Geotech. J.* **2010**, *47*, 1288–1298. [CrossRef]
56. Gu, X.; Yang, J.; Huang, M. Laboratory measurements of small strain properties of dry sands by bender element. *Soils Found.* **2013**, *53*, 735–745. [CrossRef]
57. Hoyos, L.R.; Suescún-Florez, E.A.; Puppala, A.J. Stiffness of intermediate unsaturated soil from simultaneous suction-controlled resonant column and bender element testing. *Eng. Geol.* **2015**, *188*, 10–28. [CrossRef]
58. Chong, S.-H.; Kim, J.-W.; Cho, G.-C. Rock mass dynamic test apparatus for estimating the strain-dependent dynamic properties of jointed rock masses. *Geotech. Test. J.* **2014**, *37*, 311–318. [CrossRef]
59. Perino, A.; Barla, G. Resonant column apparatus tests on intact and jointed rock specimens with numerical modelling validation. *Rock. Mech. Rock. Eng.* **2015**, *48*, 197–211. [CrossRef]
60. Sebastian, R.; Sitharam, T. Long-wavelength propagation of waves in jointed rocks-study using resonant column experiments and model material. *Geomech. Geoengin.* **2016**, *11*, 281–296. [CrossRef]
61. Abbas, H.A.; Mohamed, Z.; Mohd-Nordin, M.M. Characterization of the body wave anisotropy of an interbedded sandstone-shale at multi orientations and interlayer ratios. *Geotech. Geol. Eng.* **2022**, *40*, 3413–3429. [CrossRef]
62. Heisey, J.; Stokoe, K.; Meyer, A. Moduli of pavement systems from spectral analysis of surface waves. *Transp. Res. Rec.* **1982**, *852*, 147.
63. Palmer, D. *The Generalized Reciprocal Method of Seismic Refraction Interpretation*; Society of Exploration Geophysicists: Tulsa, OK, USA, 1980.
64. Schlumberger. *Log Interpretation Principles/Applications*; Schlumberger Educational Services: Houston, TX, USA, 1991.
65. Grosmangin, M.; Kokesh, P.; Majani, P. A sonic method for analyzing the quality of cementation of borehole casings. *J. Pet. Technol.* **1961**, *13*, 165–171. [CrossRef]
66. Maries, G.; Malehmir, A.; Bäckström, E.; Schön, M.; Marsden, P. Downhole physical property logging for iron-oxide exploration, rock quality, and mining: An example from central Sweden. *Ore Geol. Rev.* **2017**, *90*, 1–13. [CrossRef]
67. Tao, G.; He, F.; Yue, W.; Li, L. Processing of array sonic logging data with multi-scale STC technique. In Proceedings of the 69th EAGE Conference and Exhibition Incorporating SPE EUROPEC 2007, London, UK, 11–14 June 2007. cp-27-00158.
68. Kurkjian, A.; Lang, S.; Hsu, K. Slowness estimation from sonic logging waveforms. *Geoexploration* **1991**, *27*, 215–256. [CrossRef]
69. Stokoe, K.H.; Woods, R.D. In situ shear wave velocity by cross-hole method. *J. Soil Mech. Found. Div.* **1972**, *98*, 443–460. [CrossRef]
70. *D4428/D4428M-07*; Standard Test Methods for Crosshole Seismic Testing. ASTM International: West Conshohocken, PA, USA, 2014. [CrossRef]
71. Miller, P.K.; Ryden, N.; Tinkey, Y.; Olson, L.D. A comparison of shear wave velocities obtained from the crosshole seismic, spectral analysis of surface waves and multiple impacts of surface waves methods. In Proceedings of the 21st EEGS Symposium on the Application of Geophysics to Engineering and Environmental Problems, Philadelphia, PA, USA, 6–10 April 2008; cp-177-00112. Available online: https://www.pcte.com.au/images/pdf/crosshole-sonic-logging/Crosshole-Sonic-Logging-paper.pdf (accessed on 31 October 2023).
72. Park, C.B.; Miller, R.D.; Xia, J. Imaging dispersion curves of surface waves on multi-channel record. In *SEG Technical Program Expanded Abstracts 1998*; Society of Exploration Geophysicists: Houston, TX, USA, 1998; pp. 1377–1380.
73. Park, C.B.; Miller, R.D.; Xia, J. Multichannel analysis of surface waves. *Geophysics* **1999**, *64*, 800–808. [CrossRef]
74. Terry, T.; Woeller, D.; Robertson, P. Engineering Soil Parameters from Seismic Cone Penetrometer Tests-An Overview. In Proceedings of the 9th EEGS Symposium on the Application of Geophysics to Engineering and Environmental Problems, Keystone, CO, USA, 28 April–2 May 1996; cp-205-00132.

75. Campanella, R.; Robertson, P.; Gillespie, D. Seismic cone penetration test. In Proceedings of the Use of In Situ Tests in Geotechnical Engineering, Blacksburg, Virginia, 23–25 June 1986; pp. 116–130.
76. *D7400/D7400M-19*; Standard Test Methods for Downhole Seismic Testing. ASTM International: West Conshohocken, PA, USA, 2019. [CrossRef]
77. Campanella, R.; Stewart, W. Seismic cone analysis using digital signal processing for dynamic site characterization. *Can. Geotech. J.* **1992**, *29*, 477–486. [CrossRef]
78. Butcher, A.; Campanella, R.; Kaynia, A.; Massarsch, K. Seismic cone downhole procedure to measure shear wave velocity–A guideline prepared by ISSMGE TC10: Geophysical Testing in Geotechnical Engineering. In Proceedings of the XVIth International Conference on Soil Mechanics and Geotechnical Engineering, Osaka, Japan, 12–16 September 2005.
79. Jafari, M.K.; Shafiei, A.; Razmkhah, A. Dynamic properties of fine grained soils in south of Tehran. *J. Seis. Earthq. Eng.* **2002**, *4*, 25–35.
80. Leparoux, D.; Grandjean, G.; Bitri, A. Underground cavities detection using seismic Rayleigh waves. In Proceedings of the 5th EEGS-ES Meeting, Budapest, Hungary, 6–9 September 1999. cp-35-00151.
81. Upom, M.R.A.; Alel, M.N.A.; Ab Kadir, M.A.; Yuzir, A. Prediction of shear wave velocity in underground layers using Particle Swarm Optimization. In *IOP Conference Series: Materials Science and Engineering, Proceedings of the 11th International Conference on Geotechnical Engineering in Tropical Regions (GEOTROPIKA) and 1st International Conference on Highway and Transportation Engineering (ICHITRA), Kuala Lumpur, Malaysia, 27–28 February 2019*; IOP Publishing: Bristol, UK, 2019; p. 012012.
82. Al-Jeznawi, D.; Sadik, L.; Al-Janabi, M.A.Q.; Alzabeebee, A.; Hajjat, J.; Keawsawasvong, S. Developing Vs-NSPT Prediction Models Using Bayesian Framework. *Transp. Infrastruct. Geotechnol.* **2023**, *10*. [CrossRef]
83. Ghazi, A.; Moghadas, N.H.; Sadeghi, H.; Ghafoori, M.; Lashkaripur, G.R. Empirical relationships of shear wave velocity, SPT-N value and vertical effective stress for different soils in Mashhad, Iran. *Ann. Geophys.* **2015**, *58*, 2015. [CrossRef]
84. Gautam, D. Empirical correlation between uncorrected standard penetration resistance (N) and shear wave velocity (Vs) for Kathmandu Valley, Nepal. *Geomat. Nat. Hazards Risk* **2017**, *8*, 496–508. [CrossRef]
85. Daag, A.S.; Halasan, O.P.C.; Magnaye, A.A.T.; Grutas, R.N.; Solidum, R.U., Jr. Empirical correlation between standard penetration resistance (SPT-N) and Shear Wave Velocity (Vs) for soils in Metro Manila, Philippines. *Appl. Sci.* **2022**, *12*, 8067. [CrossRef]
86. Hossain, M.B.; Rahman, M.M.; Haque, M.R. Empirical correlation between shear wave velocity (Vs) and uncorrected standard penetration resistance (SPT-N) for Dinajpur District, Bangladesh. *J. Nat.* **2021**, *3*, 25–29. [CrossRef]
87. Naik, S.P.; Patra, N.R.; Malik, J.N. Spatial distribution of shear wave velocity for late quaternary alluvial soil of Kanpur city, Northern India. *Geotech. Geol. Eng.* **2014**, *32*, 131–149. [CrossRef]
88. Kirar, B.; Maheshwari, B.K.; Muley, P. Correlation between shear wave velocity (Vs) and SPT resistance (N) for Roorkee region. *Int. J. Geosynth. Ground Eng.* **2016**, *2*, 9. [CrossRef]
89. Fatehnia, M.; Amirinia, G. A review of genetic programming and artificial neural network applications in pile foundations. *Int. J. Geo-Eng.* **2018**, *9*, 2. [CrossRef]
90. Esfehanizadeh, M.; Nabizadeh, F.; Yazarloo, R. Correlation between standard penetration (N SPT) and shear wave velocity (Vs) for young coastal sands of the Caspian Sea. *Arab. J. Geosci.* **2015**, *8*, 7333–7341. [CrossRef]
91. Maheshwari, B.K.; Mahajan, A.; Sharma, M.L.; Paul, D.; Kaynia, A.; Lindholm, C. Relationship between shear velocity and SPT resistance for sandy soils in the Ganga basin. *Int. J. Geotech. Eng.* **2013**, *7*, 63–70. [CrossRef]
92. Mhaske, S.Y.; Choudhury, D. Geospatial contour mapping of shear wave velocity for Mumbai city. *Nat. Hazards* **2011**, *59*, 317–327. [CrossRef]
93. Uma Maheswari, R.; Boominathan, A.; Dodagoudar, G. Use of surface waves in statistical correlations of shear wave velocity and penetration resistance of Chennai soils. *Geotech. Geol. Eng.* **2010**, *28*, 119–137. [CrossRef]
94. Dikmen, Ü. Statistical correlations of shear wave velocity and penetration resistance for soils. *J. Geophys. Eng.* **2009**, *6*, 61–72. [CrossRef]
95. Hanumantharao, C.; Ramana, G. Dynamic soil properties for microzonation of Delhi, India. *J. Earth Syst. Sci.* **2008**, *117*, 719–730. [CrossRef]
96. Hasancebi, N.; Ulusay, R. Empirical correlations between shear wave velocity and penetration resistance for ground shaking assessments. *Bull. Eng. Geol. Environ.* **2007**, *66*, 203–213. [CrossRef]
97. Kiku, H. In-situ penetration tests and soil profiling in Adapazari, Turkey. In Proceedings of the 15th ICSMGE TC4 Satellite Conference on Lessons Learned from Recent Strong Earthquakes, Istanbul, Turkey, 25 August 2001; pp. 259–265.
98. Jafari, M.; Asghari, A.; Rahmani, I. Empirical correlation between shear wave velocity (Vs) and SPT-N value for south of Tehran soils. In Proceedings of the 4th International Conference on Civil Engineering, Tehran, Iran, 4–6 May 1997.
99. Kanai, K.; Tanaka, T.; Morishita, T.; Osada, K. Observation of microtremors, XI: Matsushiro earthquake swarm areas. *Bull. Earthq. Res. Inst.* **1966**, *4*, 1297–1333.
100. Raptakis, D.; Anastasiadis, S.; Pitilakis, K.; Lontzetidis, K. Shear wave velocities and damping of Greek natural soils. In Proceedings of the 10th European Conference on Earthquake Engineering, Vienna, Austria, 28 August–2 September 1994.
101. Athanasopoulos, G. Empirical correlations Vso-NSPT for soils of Greece: A comparative study of reliability. *WIT Trans.* **1970**, *15*, 8. [CrossRef]
102. Pitilakis, K.; Anastasiadis, A.; Raptakis, D. Field and laboratory determination of dynamic properties of natural soil deposits. In Proceedings of the 10th World Conference on Earthquake Engineering, Madrid, Spain, 19–24 July 1992; pp. 1275–1280.

103. Yokota, K.; Imai, T.; Konno, M. Dynamic deformation characteristics of soils determined by laboratory tests. *OYO Tec. Rep.* **1981**, *3*, 13–37.
104. Imai, T.; Yoshimura, Y. Elastic wave velocity and soil properties in soft soil. *Tsuchito-Kiso* **1970**, *18*, 17–22.
105. Okamoto, T.; Kokusho, T.; Yoshida, Y.; Kusuonoki, K. Comparison of surface versus subsurface wave source for P–S logging in sand layer. In Proceedings of the 44th Annual Conference of JSCE, Tokyo, Japan, October 1989; pp. 996–997. Available online: https://scholar.google.com/citations?view_op=view_citation&hl=en&user=EJwYxd8AAAAJ&cstart=20&pagesize=80&citation_for_view=EJwYxd8AAAAJ:u-coK7KVo8oC (accessed on 31 October 2023).
106. Jinan, Z. Correlation between seismic wave velocity and the number of blow of SPT and depth. *Chin. J. Geotech. Eng.* **1987**, *12*, 92–100.
107. Fumal, T.; Tinsley, J.; Ziony, J. *Mapping Shear-Wave Velocities of Near-Surface Geologic Materials*; US Geological Survey Professional Paper; US Geological Survey: Reston, VA, USA, 1985; pp. 101–126.
108. Sykora, D.W. *Correlations of In Situ Measurements in Sands of Shear Wave Velocity, Soil Characteristics, and Site Conditions*; University of Texas at Austin: Austin, TX, USA, 1983.
109. Seed, H.B.; Idriss, I.M.; Arango, I. Evaluation of liquefaction potential using field performance data. *J. Geotech. Eng.* **1983**, *109*, 458–482. [CrossRef]
110. Imai, T.; Tonouchi, K. Correlation of N-value with S-wave velocity. In Proceedings of the Symposium on Penetration Testing Proceedings of Second European, Amsterdam, The Netherlands, 24–27 May 1982; p. 72.
111. Seed, H.B.; Idriss, I. Evaluation of liquefaction potential sand deposits based on observation of performance in previous earthquakes. In Proceedings of the ASCE National Convention (MO), St. Louis, MI, USA, 26–30 October 1981; pp. 481–544.
112. JRA. *Specification and Interpretation of Bridge Design for Highway—Part V: Resilient Design*; Japan Racing Association: Minato City, Tokyo, 1980.
113. Ohta, Y.; Goto, N. Empirical shear wave velocity equations in terms of characteristic soil indexes. *Earthq. Eng. Struct. Dyn.* **1978**, *6*, 167–187. [CrossRef]
114. Imai, T. P and S wave velocities of the ground in Japan. In Proceedings of the 9th ICSMFE, Tokyo, Japan, 10–15 July 1977; pp. 257–260.
115. Imai, T.; Fumoto, H.; Yokota, K. The relation of mechanical properties of soil to P- and S- wave velocities in Japan. In Proceedings of the 4th Japan Earthquake Engineering Symposium, Tokyo, Japan, 26–28 November 1975; pp. 89–96.
116. Imai, T.; Yoshimura. *The Relation of Mechanical Properties of Soils to P- and S-Waves Velocities for Soil in Japan*; Urana Research Institute, OYO Corporation: Tokyo, Japan, 1967. Available online: https://www.scirp.org/reference/ReferencesPapers?ReferenceID=1056371 (accessed on 31 October 2023).
117. Ohsaki, Y.; Iwasaki, R. On dynamic shear moduli and Poisson's ratios of soil deposits. *Soils Found.* **1973**, *13*, 61–73. [CrossRef]
118. Ohta, Y.; Goto, N.; Kagami, H.; Shiono, K. Shear wave velocity measurement during a standard penetration test. *Earthq. Eng. Struct. Dyn.* **1978**, *6*, 43–50. [CrossRef]
119. Fujiwara, T. Estimation of ground movements in actual destructive earthquakes. In Proceedings of the Fourth European Symposium on Earthquake Engineering, London, UK, 5–7 September 1972; pp. 125–132.
120. Ohba, S.; Toriumi, I. Dynamic response characteristics of Osaka Plain. In Proceedings of the Annual Meeting AIJ, Tokyo, Japan, 5–7 December 1970.
121. Shibata, T. Analysis of liquefaction of saturated sand during cyclic loading Disaster. *Bull. Disaster Prev. Res. Inst.* **1970**, *13*, 63–70.
122. Jiang, R.; Ji, Z.; Mo, W.; Wang, S.; Zhang, M.; Yin, W.; Wang, Z.; Lin, Y.; Wang, X.; Ashraf, U. A novel method of deep learning for shear velocity prediction in a tight sandstone reservoir. *Energies* **2022**, *15*, 7016. [CrossRef]
123. Zhang, Y.; Zhang, C.; Ma, Q.; Zhang, X.; Zhou, H. Automatic prediction of shear wave velocity using convolutional neural networks for different reservoirs in Ordos Basin. *J. Pet. Sci. Eng.* **2022**, *208*, 109252. [CrossRef]
124. Allawi, R.H.; Al-Jawad, M.S. An empirical correlations to predict shear wave velocity at southern Iraq oilfield. *J. Pet. Res. Stud.* **2022**, *12*, 1–14. [CrossRef]
125. Miah, M.I. Improved prediction of shear wave velocity for clastic sedimentary rocks using hybrid model with core data. *J. Rock. Mech. Geotech. Eng.* **2021**, *13*, 1466–1477. [CrossRef]
126. Poulos, H.G. Tall building foundations: Design methods and applications. *Innov. Infrastruct. Solut.* **2016**, *1*, 10. [CrossRef]
127. Gkeli, E.; Tipler, J. Earthquake Geotechnical Engineering Practice. Module 5: Ground Improvement of Soils Prone to Liquefaction. 2021. Available online: https://www.building.govt.nz/assets/Uploads/building-code-compliance/b-stability/b1-structure/geotechnical-guidelines/module-5-geotech-ground-improvement-version-1.pdf (accessed on 29 November 2021).
128. Galupino, J.; Dungca, J. Estimating Liquefaction Susceptibility Using Machine Learning Algorithms with a Case of Metro Manila, Philippines. *Appl. Sci.* **2023**, *13*, 6549. [CrossRef]
129. Ares, A.F.; Fatehi, A. Development of probabilistic seismic hazard analysis for international sites, challenges and guidelines. *Nucl. Eng. Des.* **2013**, *259*, 222–229. [CrossRef]
130. Liu, W.; Shan, M.; Zhang, S.; Zhao, X.; Zhai, Z. Resilience in infrastructure systems: A comprehensive review. *Buildings* **2022**, *12*, 759. [CrossRef]
131. Fang, Q.; Wang, G.; Du, J.; Liu, Y.; Zhou, M. Prediction of tunnelling induced ground movement in clay using principle of minimum total potential energy. *Tunn. Undergr. Space Technol.* **2023**, *131*, 104854. [CrossRef]

132. Tatsuoka, F.; Tateyama, M.; Aoki, H.; Watanabe, K. Bridge abutment made of cement-mixed gravel back-fill. In *Elsevier Geo-Engineering Book Series*; Elsevier: Amsterdam, The Netherlands, 2005; Volume 3, pp. 829–873.
133. Krinitzsky, E.L. Deterministic versus probabilistic seismic hazard analysis for critical structures. *Eng. Geol.* **1995**, *40*, 1–7. [CrossRef]
134. Ebrahimi, A.; Izadpanahi, A.; Ebrahimi, P.; Ranjbar, A. Estimation of shear wave velocity in an Iranian oil reservoir using machine learning methods. *J. Pet. Sci. Eng.* **2022**, *209*, 109841. [CrossRef]
135. Chaudhuri, C.H.; Choudhury, D. Dynamic analysis of buried pipeline with and without barrier system subjected to underground detonation. *Def. Technol.* **2023**, *29*, 95–105. [CrossRef]
136. Yang, Y.; Zhou, W.; Jiskani, I.M.; Lu, X.; Wang, Z.; Luan, B. Slope Stability Prediction Method Based on Intelligent Optimization and Machine Learning Algorithms. *Sustainability* **2023**, *15*, 1169. [CrossRef]
137. Valencia-González, Y.; Quintero-Ramírez, A.; Lara-Valencia, L.A. A laboratory methodology for predicting variations in the geotechnical parameters of soil exposed to solid waste leachates in the field. *Results Eng.* **2022**, *14*, 100398. [CrossRef]
138. Munirwansyah, M.; Fulazzaky, M.A.; Yunita, H.; Munirwan, R.P.; Jonbi, J.; Sumeru, K. A new empirical equation of shear wave velocity to predict the different peak surface accelerations for Jakarta city. *Geod. Geodyn.* **2020**, *11*, 455–467. [CrossRef]
139. Nitta, N.; Yamakawa, M.; Hachiya, H.; Shiina, T. A review of physical and engineering factors potentially affecting shear wave elastography. *J. Med. Ultrasound* **2021**, *48*, 403–414. [CrossRef]
140. Alzahrani, H.; Abdelrahman, K.; Qaysi, S.; Al-Otaibi, N. Shear-wave velocity profiling of Jizan city, southwestern Saudi Arabia, using controlled-source spectral analysis of surface-wave measurements. *J. King Saud. Univ. Sci.* **2021**, *33*, 101592. [CrossRef]
141. Tunusluoglu, M.C. Determination of Empirical Correlations between Shear Wave Velocity and Penetration Resistance in the Canakkale Residential Area (Turkey). *Appl. Sci.* **2023**, *13*, 9913. [CrossRef]
142. Xia, J.; Miller, R.D.; Park, C.B.; Hunter, J.A.; Harris, J.B.; Ivanov, J. Comparing shear-wave velocity profiles inverted from multichannel surface wave with borehole measurements. *Soil. Dyn. Earthq. Eng.* **2002**, *22*, 181–190. [CrossRef]
143. Verstraeten, W.W.; Veroustraete, F.; Feyen, J. Assessment of evapotranspiration and soil moisture content across different scales of observation. *Sensors* **2008**, *8*, 70–117. [CrossRef]
144. Nejad, M.M.; Manahiloh, K.N.; Momeni, M.S. Random-effects regression model for shear wave velocity as a function of standard penetration test resistance, vertical effective stress, fines content, and plasticity index. *Soil. Dyn. Earthq. Eng.* **2017**, *103*, 95–104. [CrossRef]
145. Lontsi, A.M.; Ohrnberger, M.; Krüger, F. Shear wave velocity profile estimation by integrated analysis of active and passive seismic data from small aperture arrays. *Appl. Geophys.* **2016**, *130*, 37–52. [CrossRef]
146. Akin, M.K.; Kramer, S.L.; Topal, T. Empirical correlations of shear wave velocity (Vs) and penetration resistance (SPT-N) for different soils in an earthquake-prone area (Erbaa-Turkey). *Eng. Geol.* **2011**, *119*, 1–17. [CrossRef]
147. Paoletti, V. Remarks on factors influencing shear wave velocities and their role in evaluating susceptibilities to earthquake-triggered slope instability: Case study for the Campania area (Italy). *Nat. Hazards Earth Syst. Sci.* **2012**, *12*, 2147–2158. [CrossRef]
148. Das, B.M. *Principles of Foundation Engineering, Cengage Learning, 2016: Principles of Foundation Engineering*; Bukupedia: West Jakarta, Indonesia, 2016; Volume 1.
149. Idriss, I.; Boulanger, R. Semi-empirical procedures for evaluating liquefaction potential during earthquakes. *Soil Dyn. Earthq. Eng.* **2006**, *26*, 115–130. [CrossRef]
150. Robertson, P.; Wride, C. Cyclic liquefaction and its evaluation based on SPT and CPT: Seismic Short Course on Evaluation and Mitigation of Earthquake Induced Liquefaction Hazards. In Proceedings of the NCEER Workshop, San Francisco, CA, USA, 31 December 1997.
151. Seed, H.B. Soil Moduli and Damping Factors for Dynamic Response Analyses. Report 1970, EERC 70-10. Available online: https://cir.nii.ac.jp/crid/1571135649476004864 (accessed on 31 October 2023).
152. Coduto, D.P.; Yeung, M.C.R.; Kitch, W.A. *Geotechnical Engineering: Principles and Practices*, 2nd ed.; Pearson: London, UK, 2011. Available online: https://www.researchgate.net/publication/261287253_Geotechnical_Engineering_Principles_and_Practices (accessed on 31 October 2023).
153. Tomlinson, M.; Woodward, J. *Pile Design and Construction Practice*; CRC Press: London, UK, 2014.
154. Whitman, R.V.; Liao, S.S. Analytical methods for predicting response of underground structures to earthquakes. *Earthq. Eng. Struct. Dyn.* **1985**, *13*, 411–427.